

Deconfinement and degrees of freedom in pp and $A - A$ collisions at LHC energies

Aditya N Mishra^{1,2}, Guy Paić¹, C. Pajares³, R. P. Scharenberg⁴ and B. K. Srivastava⁴

¹*Instituto de Ciencias Nucleares, Universidad Nacional Autónoma de México,
Apartado Postal 70-543, México Distrito Federal 04510, México*

²*Wigner Research Center for Physics, H-1121 Budapest, Hungary*

³*Departamento de Física de Partículas, Universidade de Santiago de Compostela and
Instituto Galego de Física de Atlas Enerxías (IGFAE), 15782 Santiago, de Compostela, Spain*

⁴*Department of Physics and Astronomy, Purdue University, West Lafayette, IN-47907, USA*

(Dated: July 27, 2021)

We present the extraction of the temperature by analyzing the charged particle transverse momentum spectra in lead-lead (Pb-Pb) and proton-proton (**pp**) collisions at LHC energies from the ALICE Collaboration using the Color String Percolation Model (CSPM). From the measured energy density ϵ and the temperature T the dimensionless quantity ϵ/T^4 is obtained to get the degrees of freedom (DOF), $\epsilon/T^4 = \text{DOF } \pi^2/30$. We observe for the first time a two-step behavior in the increase of DOF, characteristic of deconfinement, above the hadronization temperature at temperature ~ 210 MeV for both Pb-Pb and **pp** collisions and a sudden increase to the ideal gas value of ~ 47 corresponding to three quark flavors in the case of Pb-Pb collisions.

PACS numbers: 25.75.-q, 25.75.Gz, 25.75.Nq, 12.38.Mh

I. INTRODUCTION

The Quantum Chromodynamics (QCD) phase diagram is closely related to the history of the universe and can be probed by heavy ion collisions. Of particular interest in the heavy ion collision experiments are the details of the deconfinement and chiral transitions which determine the QCD phase diagram. One of the main challenges of the field is to simultaneously determine the temperature and the energy density of the matter produced in a collision and hence the number of thermodynamic degrees of freedom (DOF) [1]. The present work explores the initial stage of high energy collisions at LHC energies analyzing the published ALICE data [2, 3] on the transverse momentum (p_t) spectra of charged particles using the framework of the clustering of color sources (CSPM) [4]. This approach has been successfully used to describe the initial stages in the soft region in high energy nucleus-nucleus and nucleon-nucleon collisions [4–9]. The CSPM is in fact different from the hydrodynamics picture and is more in line with other studies where the interaction among strings [10–12] or the domain color structure [13, 14] is taken into account. The determination of the DOF requires the measurement of the initial thermalized (maximum entropy) temperature and the initial energy density at time ~ 1 fm/c of the hot matter produced in high energy A-A and pp collisions. Lattice Quantum Chromo Dynamics simulations (LQCD) indicate that the non-perturbative region of hot QCD matter extends up to temperature of 400 MeV, well above the universal hadronization temperature [15].

II. CLUSTERING OF COLOR SOURCES AND PERCOLATION

Multiparticle production is currently described in terms of color strings stretched between the projectile and the target, which decay into new strings and subsequently hadronize to produce observed hadrons. Color strings may be viewed as small areas in the transverse plane filled with color field created by colliding partons. With growing energy and size of the colliding system, the number of strings grows, and they start to overlap, forming clusters, in the transverse plane very much similar to disks in two dimensional percolation theory [16]. At a certain critical density $\xi_c \sim 1.2$ a macroscopic cluster appears that marks the percolation phase transition. For nuclear collisions, this density corresponds to $\xi = N_s \frac{S_1}{S_A}$ where N_s is the total number of strings created in the collision, each one of area $S_1 = \pi r_0^2$ and S_A corresponds to nuclear overlap area, with $r_0 \approx 0.2$ fm. This is the Color String Percolation Model (CSPM) [17, 18].

The interaction between strings occurs forming clusters when they overlap and the general result, due to the SU(3) random summation of charges, is a reduction in multiplicity and an increase in the average transverse momentum squared, $\langle p_t^2 \rangle$. The strings decay into new ones through color neutral $q - \bar{q}$ pairs production. The Schwinger QED₂ string breaking mechanism produces these $q - \bar{q}$ pairs at time $\tau_{pro} \sim 1$ fm/c, which subsequently hadronize to produce the observed hadrons [19]. Schwinger mechanism has also been used in the decay of color flux tubes produced by the quark-gluon plasma for

modeling the initial stages in heavy ion collisions [20, 21].

The combination of the string density dependent cluster formation and the 2D percolation clustering phase transition, are the basic elements of the non-perturbative CSPM. The percolation theory governs the geometrical pattern of string clustering. Its observable implications, however, require the introduction of some dynamics in order to describe the behavior of the cluster formed by several overlapping clusters. We assume that a cluster of n strings that occupies an area of S_n behaves as a single color source with a higher color field \vec{Q}_n corresponding to the vectorial sum of the color charges of each individual string \vec{Q}_1 . The resulting color field covers the area of the cluster. As $\vec{Q}_n = \sum_1^n \vec{Q}_1$, and the individual string colors may be oriented in an arbitrary manner respective to each other, the average $\vec{Q}_{1i}\vec{Q}_{1j}$ is zero, and $\vec{Q}_n^2 = n\vec{Q}_1^2$. Knowing the color charge, one can compute the multiplicity μ_n and the mean transverse momentum squared $\langle p_t^2 \rangle_n$ of the particles produced by a cluster, which are proportional to the color charge and color field, respectively [18]

$$\mu_n = \sqrt{\frac{nS_n}{S_1}}\mu_0; \quad \langle p_t^2 \rangle_n = \sqrt{\frac{nS_1}{S_n}}\langle p_t^2 \rangle_1, \quad (1)$$

where μ_0 and $\langle p_t^2 \rangle_1$ are the mean multiplicity and transverse momentum squared of particles produced from a single string with a transverse area $S_1 = \pi r_0^2$ with $r_0 = 0.2$ fm [4]. For strings just touching each other $S_n = nS_1$, and $\mu_n = n\mu_0$, $\langle p_t^2 \rangle_n = \langle p_t^2 \rangle_1$. When strings fully overlap, $S_n = S_1$ and therefore $\mu_n = \sqrt{n}\mu_0$ and $\langle p_t^2 \rangle_n = \sqrt{n}\langle p_t^2 \rangle_1$, so that the multiplicity is maximally suppressed and the $\langle p_t^2 \rangle_n$ is maximally enhanced. This implies a simple relation between the multiplicity and transverse momentum $\mu_n \langle p_t^2 \rangle_n = n\mu_0 \langle p_t^2 \rangle_1$, which means conservation of the total transverse momentum produced. In the thermodynamic limit, one obtains the average value of nS_1/S_n for all the clusters [17, 18]

$$\left\langle \frac{nS_1}{S_n} \right\rangle = \frac{\xi}{1 - e^{-\xi}} \equiv \frac{1}{F(\xi)^2} \quad (2)$$

where $F(\xi)$ is the color suppression factor by which the overlapping strings reduce the net color charge of the strings. With $F(\xi) \rightarrow 1$ as $\xi \rightarrow 0$ and $F(\xi) \rightarrow 0$ as $\xi \rightarrow \infty$, where $\xi = \frac{N_s S_1}{S_N}$ is the percolation density parameter. Eq. (1) can be written as $\mu_n = nF(\xi)\mu_0$ and $\langle p_t^2 \rangle_n = \langle p_t^2 \rangle_1/F(\xi)$. It is worth noting that CSPM is a saturation model similar to the Color Glass Condensate (CGC), where $\langle p_t^2 \rangle_1/F(\xi)$ plays the same role as the saturation momentum scale Q_s^2 in the CGC model [22, 23].

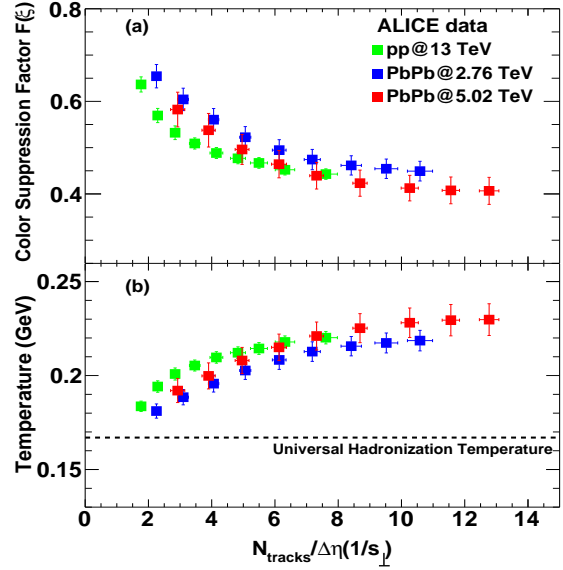


FIG. 1: (a). Color Suppression Factor $F(\xi)$ in Pb-Pb and \mathbf{pp} collisions vs $N_{tracks}/\Delta\eta$ scaled by the transverse area S_\perp . N_{tracks} is the charged particle multiplicity in the pseudorapidity range $|\eta| < 0.8$ with $\Delta\eta = 1.6$ units. For \mathbf{pp} collisions S_\perp is multiplicity dependent as obtained from IP-Glasma model [28]. In case of Pb-Pb collisions the nuclear overlap area was obtained using the Glauber model [31]. (b). Temperature vs $N_{tracks}/\Delta\eta$ scaled by S_\perp from Pb-Pb and \mathbf{pp} collisions. The line ~ 165 MeV is the universal hadronization temperature [35].

III. EXTRACTION OF THE COLOR SUPPRESSION FACTOR $F(\xi)$

In the present work we have extracted $F(\xi)$ in Pb-Pb collisions using ALICE data from the transverse momentum spectra of charged particles at $\sqrt{s_{NN}} = 2.76$ and 5.02 TeV at various centralities [3]. In case of \mathbf{pp} collisions at $\sqrt{s} = 13$ TeV, $F(\xi)$ has been obtained in high multiplicity events [2]. Only the softer sector of the spectra with p_t in the range 0.15-1.0 GeV/c is considered. We have checked that the extension of the soft range up to $p_t = 2$ GeV/c does not change significantly our results. To evaluate the initial value of $F(\xi)$ from data a parameterization of the experimental data of p_t distribution in low energy \mathbf{pp} collisions at $\sqrt{s} = 200$ GeV, where strings have low overlap probability, was used [5]. The charged particle spectrum is described by a power-law [4]

$$d^2 N_c / dp_t^2 = a / (p_0 + p_t)^\alpha, \quad (3)$$

where a is the normalization factor, p_0 and α are fitting parameters with $p_0 = 1.98$ and $\alpha = 12.87$ [5]. This parameterization is used both in Pb-Pb, and in \mathbf{pp} collisions to take into account the interactions of the strings [4]. The parameter p_0 in Eq. (3) is for

independent strings and gets modified

$$p_0 \rightarrow p_0 \left(\frac{\langle nS_1/S_n \rangle^{mod}}{\langle nS_1/S_n \rangle_{pp}} \right)^{1/4}, \quad (4)$$

In **pp** collisions at low energies only two strings are exchanged with low probability of interactions, so that $\langle nS_1/S_n \rangle_{pp} \approx 1$, which transforms Eq. (3) into

$$\frac{d^2 N_c}{dp_t^2} = \frac{a}{(p_0 \sqrt{1/F(\xi)^{mod}} + p_t)^\alpha}, \quad (5)$$

where $F(\xi)^{mod}$ is the modified color suppression factor and is used in extracting $F(\xi)$ both in Pb-Pb and **pp** in high multiplicity events. The color suppression factor $F(\xi)$ encodes the effect of the interaction among strings once they overlap. In the thermodynamic limit $F(\xi)$ is related to the string density ξ [4]

$$F(\xi) = \sqrt{\frac{1 - e^{-\xi}}{\xi}}. \quad (6)$$

The partons produced in the decay of a cluster in-

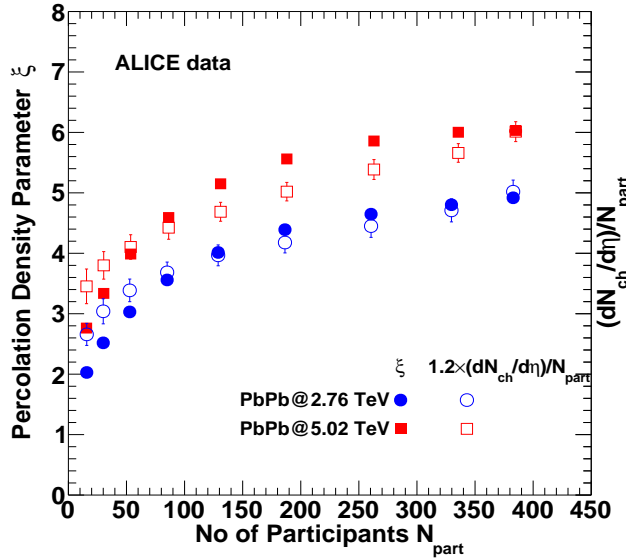


FIG. 2: ξ as a function of N_{part} for Pb-Pb collisions at $\sqrt{s_{NN}} = 2.76$ and 5.02 TeV. $(dN_{ch}/d\eta)/N_{part}$ is also shown on the figure for comparison with ξ .

teract with the color of the clusters in their way out the collision surface, modifying their momenta. This reproduces the experimental harmonics of the azimuthal asymmetry observed in **pp**, **p - A**, and **A-A** collisions. The size of the momentum modification is small and do not change the p_t distribution. [24–27].

IV. RESULTS AND DISCUSSIONS

Figure 1(a) shows $F(\xi)$ as a function of $N_{tracks}/\Delta\eta$ scaled by the transverse area S_\perp for both Pb-Pb and **pp** collisions. The error on $F(\xi)$ is $\sim 3\%$ and is obtained with changing the fitting range of the transverse momentum spectra. For **pp** collisions S_\perp is multiplicity dependent according to the IP-Glasma model [28–30]. In the case of Pb-Pb collisions the nuclear overlap area was obtained using the Glauber model [31]. A universal scaling behavior is observed in hadron-hadron and nucleus-nucleus collisions. The percolation density parameter ξ is obtained from $F(\xi)$ using the relation Eq. (6) is shown in Fig. 2 as a function of number of participants N_{part} for Pb-Pb collisions at $\sqrt{s_{NN}} = 2.76$ and 5.02 TeV. It is observed that ξ rises slowly at higher N_{part} . This behavior is similar to measured $(dN_{ch}/d\eta)/N_{part}$ as shown in Fig. 2.

The connection between $F(\xi)$ and the temperature $T(\xi)$ involves the Schwinger QED₂ mechanism (SM) for particle production. The Schwinger distribution for mass less particles is expressed in terms of p_t^2 [4, 32]

$$dn/dp_t^2 \sim e^{-\pi p_t^2/x^2} \quad (7)$$

where the average value of the string tension is $\langle x^2 \rangle$. The tension of the macroscopic cluster fluctuates around its mean value because the chromoelectric field is not constant. The origin of the string fluctuation is related to the stochastic nature of the QCD vacuum. Since the average value of the color field strength must vanish, it cannot be constant but changes randomly from point to point [33, 34]. Such fluctuations lead to a Gaussian distribution of the string tension and transforms SM into the thermal distribution [33]

$$\frac{dn}{dp_t^2} \sim \exp\left(-p_t \sqrt{\frac{2\pi}{\langle x^2 \rangle}}\right), \quad (8)$$

with $\langle x^2 \rangle = \pi \langle p_t^2 \rangle_1 / F(\xi)$. The temperature is expressed as [5, 32]

$$T(\xi) = \sqrt{\frac{\langle p_t^2 \rangle_1}{2F(\xi)}}. \quad (9)$$

We adopt the point of view that the universal hadronization temperature is a good measure of the upper end of the cross over phase transition temperature T_h [35]. The single string average transverse momentum $\langle p_t^2 \rangle_1$ is calculated at $\xi_c = 1.2$ with the universal hadronization temperature $T_h = 167.7 \pm 2.6$ MeV [35]. This gives $\sqrt{\langle p_t^2 \rangle_1} = 207.2 \pm 3.3$ MeV.

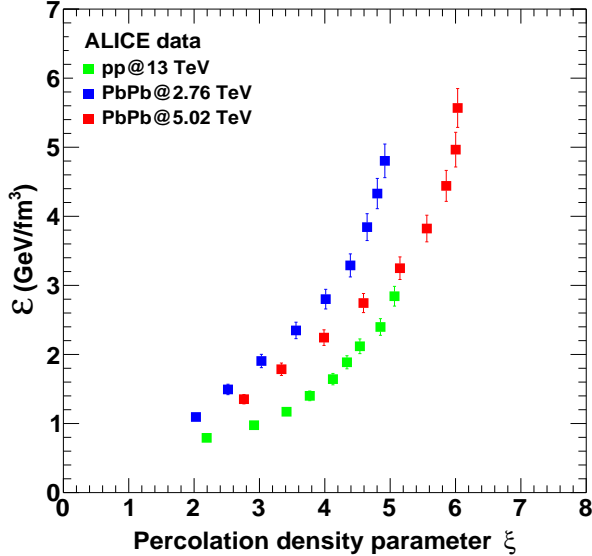


FIG. 3: Energy density ε ($\text{GeV}/f\text{m}^3$) as a function of string density ξ for Pb-Pb and **pp** collisions at LHC energies. The energy density is obtained using Eq. (10) and ξ is obtained using Eq. (6).

Figure 1(b) shows a plot of temperature as a function of $N_{\text{tracks}}/\Delta\eta$ scaled by S_{\perp} . N_{tracks} is the charged particle multiplicity in the pseudorapidity range $|\eta| < 0.8$ with $\Delta\eta = 1.6$ units. The temperature dependence, for the systems investigated, falls on a universal curve as a function of the scaled multiplicity. The horizontal line at ~ 165 MeV is the universal hadronization temperature obtained from the systematic comparison of the statistical thermal model parametrization of hadron abundances measured in high energy e^+e^- , **pp**, and A-A collisions [35]. In Fig.1(b) the temperatures obtained for Pb-Pb and **pp** are above the hadronization temperature indicating deconfinement.

Recently, it has been suggested that fast thermalization in A-A and **pp** collisions can occur through the existence of an event horizon due to a rapid deceleration of the colliding nuclei [36, 37]. The thermalization in this case is due to the Hawking-Unruh effect [36, 38–40]. In CSPM the strong color field inside the large cluster produces deceleration of the primary $q\bar{q}$ pair which can be seen as a thermal temperature by means of Hawking-Unruh effect [39, 40]. In the CSPM the initial local temperature determined at the string level becomes the global temperature of the initial state as the cluster spans the whole area above the percolation threshold.

The QGP according to CSPM is born in thermal equilibrium because the initial temperature is determined at the string level. Above the critical temperature $T > T_c$ the CSPM energy expands according

to the Bjorken boost invariant 1D hydrodynamics [41]

$$\varepsilon = \frac{3}{2} \frac{dN_c \langle m_t \rangle}{S_{\perp} \tau_{pro}}, \quad (10)$$

where ε is the energy density, S_{\perp} the nuclear overlap area, m_t is the transverse mass and τ_{pro} is the Schwinger production time for a boson (gluon) $\tau_{pro} = 2.45/\langle m_t \rangle$ [42]. Figure 3 shows ε as a function of ξ for Pb-Pb and **pp** collisions. We observe a slow rise of ε for low values of ξ followed by a faster rise later. This is due to the nonlinear increase in multiplicity at higher ξ values. In the case of Pb-Pb these data show a large departure of the scaling of the multiplicity per participant. This change occurs at $\xi \sim 4.2$ and ~ 5.0 for Pb-Pb at 2.76 TeV and 5.02 TeV respectively. For **pp** the jump in ε is at $\xi \sim 3.8$.

In Fig. 4 we show the results of dimensionless quantity ε/T^4 for Pb-Pb collisions at two different energies and those for **pp** at 13 TeV. The results are compared with LQCD predictions for 2+1 flavors [43, 44]. It is observed that CSPM results agree with LQCD results up to the temperature of $T \sim 210$ MeV for the Pb-Pb collisions. Beyond this temperature the ε/T^4 in CSPM rises much faster and reaches the ideal gas value of $\varepsilon/T^4 \sim 16$ at $T \sim 230$ MeV. In this region, there is a strong screening due to the large degree of overlapping of the strings, producing a faster approach to the quark gluon gas limit.

The DOF are obtained using the relation $\varepsilon/T^4 = \text{DOF} \pi^2/30$ [19]. At $T \sim 210$ MeV, $\varepsilon/T^4 \sim 11$ which corresponds to ~ 33 DOF while at $T \sim 230$ MeV there are ~ 47 DOF. It is observed that Pb-Pb at $\sqrt{s_{NN}} = 2.76$ TeV has similar features as seen at 5.02 TeV. In **pp** collisions at $\sqrt{s} = 13$ TeV only ~ 33 DOF are reached. Our results are in agreement with the conclusions obtained studying the trace anomaly in a quasi particle gluonic model [45, 46]. In this model the DOF of the free gluons are also obtained for $T \simeq 1.3T_c$ ($T_c \approx 165$ MeV).

There are several reasons that can explain the disagreement between CSPM and lattice QCD for $T > 1.3T_c$. First in A-A and pp collisions a strong magnetic field B is produced, which is larger for A-A than for pp and increases with energy. The lattice studies of the chiral phase structure of three flavor QCD in a background magnetic field show that chiral condensate and the phase transition temperature always increases with B . The transition becomes stronger and turns into a first order instead of crossover [47]. As B is higher in PbPb than in pp, we expect a higher phase transition temperature in these cases.

Recently, it has been pointed out using lattice simulations that in addition of the standard crossover

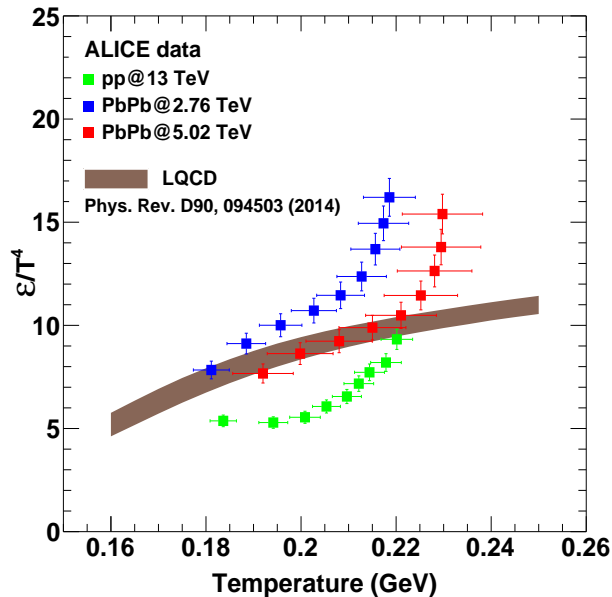


FIG. 4: Dimensionless quantity ϵ/T^4 as a function of temperature for Pb-Pb collisions at $\sqrt{s_{NN}} = 2.76$ and 5.02 TeV. **pp** at $\sqrt{s} = 13$ TeV is shown as green rectangle. The brown band corresponds to LQCD simulations [43].

phase transition at $T \sim 155$ MeV, the existence of a new infrared phase transition at temperature T , $200 < T_{IR} < 250$ MeV. In this phase, asymptotic freedom works and therefore there is no interaction. In between these two temperatures there is coexistence of the short and long distance scales [48], which supports the present observation in our work.

A new phase in QCD also has been proposed studying the Dirac operator. While confining chromo-electric interaction is distributed among all modes of Dirac operator, the chromo-magnetic interaction is located predominantly in the near zero modes. Above $T \sim 155$ MeV the near zero modes are suppressed but not the rest of the modes, surviving the chromo-electric interaction which is suppressed at higher temperature [49].

V. CONCLUSION

We have used the Color String Percolation Model (CSPM) to explore the initial stage of high energy nucleus-nucleus and nucleon-nucleon collisions and determined the thermalized initial temperature of the hot nuclear matter at an initial time ~ 1 fm/c. For the first time the temperature and the energy density of the hot nuclear matter, from the measured charged particle spectra using ALICE data for Pb-Pb collisions at $\sqrt{s_{NN}} = 2.76$ and 5.02 TeV and **pp** collisions at $\sqrt{s} = 13$, TeV have been obtained. The dimensionless quantity ϵ/T^4 is evaluated to obtain the number of degrees of freedom (DOF) of the deconfined phase. We observe two features hitherto not reported: the existence of two temperature ranges in the behavior of the Pb-Pb system DOF, and a clear departure from the LQCD results regarding the maximum number of DOF, which reaches values in agreement with the Stephan Boltzmann limit for an ideal gas of quarks and gluons.

Acknowledgments

A. M. acknowledges the post-doctoral fellowship of DGAPA UNAM. Partial support was received by DGAPA-PAPIIT IN109817 and CONACYT A1-S-16215 projects. A. M. also thanks the Hungarian National Research, Development and Innovation Office (NKFIH) under the contract numbers OTKA K120660, NKFIH 2019-2.1.11-T ET-2019-00078, and 2019-2.1.11-T ET-2019-00050. C. P. thanks the grant Maria de Maeztu Unit of excellence MDM-2016-0682 of Spain, the support of Xunta de Galicia under the project ED431C 2017 and project FPA 2017-83814 of Ministerio de Ciencia e Innovacion of Spain and FEDER. GP acknowledges the DGAPA sabbatical fellowship.

[1] W. Busza, K. Rajagopal, and W. van der Schee, Heavy ion collisions: The Big Picture, and the Big Questions, *Ann. Rev. Nucl. Part. Sci.* **68**, 339 (2018).
 [2] S. Acharya *et al.* (ALICE Collaboration), Charged particle production as a function of multiplicity and transverse sphericity in pp collisions at $\sqrt{s} = 5.02$ and 13 TeV, *Eur. Phys. J. C* **79**, 857 (2019).
 [3] S. Acharya *et al.* (ALICE Collaboration), Transverse momentum spectra and nuclear modification factors of charged particles in pp, p-Pb and Pb-Pb collisions at the LHC, *JHEP* **11**, 013 (2018).

[4] M. A. Braun, J. Dias de Deus, A. S. Hirsch, C. Pajares, R. P. Scharenberg, and B. K. Srivastava, Deconfinement and clustering of color sources in nuclear collisions, *Phys. Rep.* **599**, 1 (2015).
 [5] R. P. Scharenberg, B. K. Srivastava, and A. S. Hirsch, Percolation of color sources and the equation of state of QGP in central Au-Au collisions at $\sqrt{s_{NN}} = 200$ GeV, *Eur. Phys. J. C* **71**, 1510 (2011).
 [6] J. Dias de Deus, A. S. Hirsch, C. Pajares, R. P. Scharenberg, and B. K. Srivastava, Clustering of color sources and the shear viscosity of the QGP in heavy ion collisions at RHIC and LHC energies,

- Eur. Phys. J. C **72**, 2123 (2012).
- [7] B. K. Srivastava, Percolation approach to initial stage effects in high energy collisions, Nucl. Phys. A **926**, 142 (2014).
- [8] J. Dias de Deus, A. S. Hirsch, C. Pajares, R. P. Scharenberg, and B. K. Srivastava, Transport coefficient to trace anomaly in the clustering of color sources approach, Phys. Rev. C **93**, 024915 (2016).
- [9] R. P. Scharenberg, B. K. Srivastava, and C. Pajares, Exploring the initial stage of high multiplicity proton-proton collisions by determining the initial temperature of quark-gluon plasma, Phys. Rev. D **100**, 114040 (2019).
- [10] C. Bierlich, G. Gustafson, L. Lonnald, and A. Tarasov, Effects of overlapping strings in pp collisions, JHEP **03**, 58 (2015).
- [11] C. Bierlich, G. Gustafson, and L. Lonnald, Collectivity without plasma in hadronic collisions, Phys. Lett. B **779**, 58 (2018).
- [12] A. Ortiz Velasquez, P. Christiansen, E. Cuautle Flores, I. A. Maldonado, and G. Paic, Color reconnection and flowlike patterns in pp collisions, Phys. Rev. Lett. **111**, 042001 (2013).
- [13] M. Asakawa, S. A. Bass, and B. Muller, Center domains and their phenomenological consequences, Phys. Rev. Lett. **110**, 202301 (2013).
- [14] A. Dumitru, T. Lappi, and Y. Nara, Structure of longitudinal chromomagnetic fields in high energy collisions, Phys. Lett. B **734**, 7 (2014).
- [15] A. Bazavov, P. Petreczky and J. H. Weber, Equation of state in 2+1 flavor QCD at high temperatures, Phys. Rev. Lett. **97**, 014510 (2018).
- [16] M. B. Isichenko, Statistical topography and transport in random media, Rev. Mod. Phys. **64**, 961(1992).
- [17] M. A. Braun and C. Pajares, Implications of color-string percolation on multiplicities, correlations, and the transverse momentum, Eur. Phys. J. C **16**, 349 (2000).
- [18] M. A. Braun, F. del Moral, and C. Pajares, Percolation of strings and the relativistic energy data on multiplicity and transverse momentum distributions, Phys. Rev. C **65**, 024907 (2002).
- [19] C. Y. Wong, Introduction to high energy heavy ion collisions (World scientific company, Singapore, 1994, page 289).
- [20] R. Ryblewski and W. Florkowski, Equilibration of anisotropic quark-gluon plasma produced by decays of color flux tubes, Phys. Rev. D **88**, 034028 (2013).
- [21] M. Ruggieri et al., Modelling the early stages of relativistic heavy ion collisions: Coupling relativistic transport theory to decaying color-electric flux tubes, Phys. Rev. C **92**, 064904 (2015).
- [22] L. McLerran and R. Venugopalan, Computing quark and gluon distribution functions for very large nuclei, Phys. Rev. D **49**, 2233 (1994).
- [23] J. Dias de Deus and C. Pajares, String percolation and the GJasma, Phys. Lett. B **695**, 211 (2011).
- [24] M. A. Braun, C. Pajares, and V. V. Vecherinn, Nucl. Phys. A **906**, 4 (2013).
- [25] M. A. Braun, C. Pajares, and V. V. Vecherinn, Ridge from strings, Eur. Phys. A **51**, 44 (2015).
- [26] M. A. Braun and C. Pajares, p_t dependence of the flow coefficients for pp collisions in the color string scenario: Monte Carlo simulations, Eur. Phys. A **54**, 185 (2018).
- [27] M. A. Braun and C. Pajares, Elliptic and triangular flows in dAu collisions at 200 GeV in the fusing color string model, Eur. Phys. A **56**, 41 (2020).
- [28] L. McLerran, M. Praszalowicz, and B. Schenke, Transverse momentum of Protons, Pions and Kaons in high multiplicity pp and pA collisions: Evidence for the Color Glass Condensate ?, Nucl. Phys. A **916**, 210 (2013).
- [29] L. McLerran and P. Tribedy, Intrinsic fluctuations of the proton saturation momentum scale in high multiplicity $p+p$ collisions, Nucl. Phys. A **945**, 216 (2016).
- [30] P. Castorina et al., Universality in hadronic and nuclear collisions at high energy, Phys. Rev. C **101**, 054902 (2020).
- [31] C. Loizides, Modelling of high-energy nuclear collisions at the subnucleon level, Phys. Rev. C **94**, 024914 (2016).
- [32] J. Dias de Deus and C. Pajares, Percolation of color sources and critical temperature, Phys. Lett. B **642**, 455 (2006).
- [33] A. Bialas, Fluctuations of the string tension and transverse mass distribution, Phys. Lett. B **466**, 301 (1999).
- [34] H. G. Dosch, Gluon condensate and effective linear potential, Phys. Lett. B **190**, 177 (1987).
- [35] F. Becattini, P. Castorina, A. Milov, and H. Satz, A comparative analysis of statistical hadron production, Eur. Phys. J. C **66**, 377 (2010).
- [36] P. Castorina, D. Kharzeev, and H. Satz, Thermal hadronization and Hawking-Unruh radiation in QCD, Eur. Phys. J. C **52**, 187 (2007).
- [37] A. A. Bylinkin, D. E. Kharzeev, and A. A. Rostovtsev, The origin of thermal component in the transverse momentum spectra in high energy hadronic processes, Int. J. Mod. Phys. E **23**, 1450083 (2014).
- [38] H. Satz, Extreme states of matter in strong interaction physics: Lecture Notes in Physics. 945 (2018), Springer International Publishing AG.
- [39] S. W. Hawking, Particle creation by black holes, Math. Phys. **43**, 199 (1975).
- [40] W. G. Unruh, Notes on black-hole evaporation, Phys. Rev. D **14**, 870 (1976).
- [41] J. D. Bjorken, Highly relativistic collisions : The central rapidity region, Phys. Rev. D **27**, 140 (1983).
- [42] J. Schwinger, J. Gauge variance and mass II, Phys. Rev. **128**, 2425 (1962).
- [43] A. Bazavov, T. Bhattacharya, C. DeTar, H. -T. Ding, S. Gottlieb, R. Gupta et al. (HotQCD Collaboration), Equation of state in (2+1) flavor QCD, Phys. Rev. D **90**, 094503 (2014).
- [44] B. Borsanyi et al. (Wuppertal Collaboration), Full result for the QCD equation of state with 2+1 flavors, Phys. Lett. B **730**, 99 (2014).
- [45] P. Castorina and M. Mannarelli, Effective degrees of freedom of the quark-gluon plasma, Phys. Lett. B **644**, 336 (2007).
- [46] P. Castorina and M. Mannarelli, Effective degrees of freedom and gluon condensation in the high temperature deconfined phase, Phys. Rev. C **75**, 054901

- (2007).
- [47] H. T. Ding et al., Chiral phase structure of three flavor QCD in a background magnetic field, Phys. Rev. D **102** 054505 (2020).
- [48] A. Alexandru and I. Horváth, Possible new phase of thermal QCD, Phys. Rev. D **100**, 094507 (2019).
- [49] Three regimes of QCD, L. Ya. Glozman, Three regimes of QCD , arXiv:1907.018201.